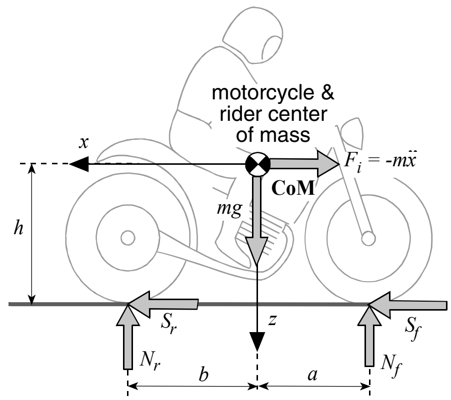

Figure 1 - simple motorcycle model

height, a and b are the center of mass distance from the front and rear wheel axles respectively, N_f and N_r are the front and the rear tire vertical loads, S_f and S_r are the front and rear braking forces, g is the acceleration due to gravity and $\ddot{x}$ is the deceleration.

While a car driver controls only the total braking force, motorcycles typically have independent front and rear brake actuators. The rider balances the rear and front braking forces according to his skill and experience. The basic problems which should be considered in order to achieve a proper repartition of the braking forces are discussed below.

LOAD TRANSFER AND REAR WHEEL LIFTING

Equations (1) give the following expressions for the tire vertical loads:

$$N_f = mg\frac{b}{a+b} + m\ddot{x}\frac{h}{a+b}$$
$$N_r = mg\frac{a}{a+b} - m\ddot{x}\frac{h}{a+b} \qquad (2)$$

These expressions show that tire loads are subjected to a dynamic load transfer proportional to the deceleration $\ddot{x}$ and to the center of mass height h. Typically h is comparable to a and b, thus the transfer load is substantial. In order to avoid rear wheel lift, the deceleration must be limited as follows:

$$\ddot{x} < g\frac{a}{h} \qquad (3)$$

TIRES SKIDDING

Another situation that must be avoided to maintain braking safety is tire skidding. Tire adherence is limited and the ratio between braking force and vertical load μ (i.e. the normalized braking force, also called braking force coefficient) must not exceed its maximum value D for both the front and rear tires [2]:

$$\mu_f = \frac{S_f}{N_f} < D_f, \qquad \mu_r = \frac{S_r}{N_r} < D_r \qquad (4)$$

As the total brake force increases, tire skidding may occur either in the front or in the rear tire depending on the braking force distribution. In order to study this phenomenon, it is useful to introduce the braking balance ρ, i.e. the ratio between the rear braking force and the total braking force, as follows:

$$\rho = \frac{S_r}{S_r + S_f} = \frac{S_r}{S_{tot}} \qquad (5)$$

By using the equations of motion (1), normalized braking force may be expressed as a function of the deceleration $\ddot{x}$ and the braking balance ρ, as follows:

$$\mu_f = (1-\rho)\frac{(a+b)\ddot{x}}{ag + h\ddot{x}}$$
$$\mu_r = \rho\frac{(a+b)\ddot{x}}{ag - h\ddot{x}} \qquad (6)$$

These expressions are represented in Figure 2 for a sport motorcycle. Normalized braking forces are limited by braking traction coefficients, dictated by the tire ground interaction. These values define a rectangular area in the (μ_f, μ_r) plane. A further constraint is the vertical line that corresponds to the rear wheel lift condition (stoppie): in this particular example this limit is reached before tire skidding and so the allowed area is reduced. Inside the allowed area, each point may be associated to a different braking maneuver.

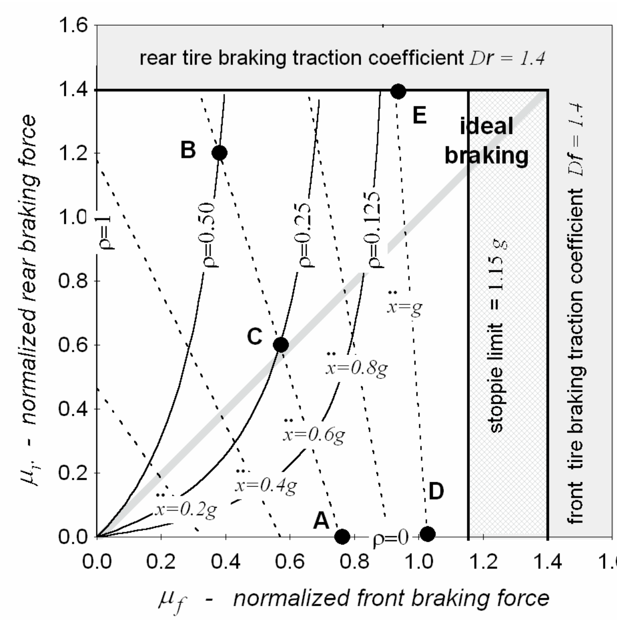

Figure 2 – distribution of the braking force
(m=274 kg, a= 0.741 m, b=0.682 m, h=0.643 m)

The dotted lines represent maneuvers at constant deceleration, whereas the solid lines represent maneuvers at constant braking balance. The horizontal axis corresponds to the use of only the front brake ($\rho = 0$), whereas the vertical axis corresponds to the use of only the rear brake ($\rho = 1$).

The constant deceleration lines are crossed by multiple braking balance lines, thus the same deceleration may be achieved by different distributions of the braking force. For example, the deceleration $\ddot{x} = 0.6g$ may be achieved using the front brake only (point A, $\rho = 0$). The corresponding value of the normalized braking force is $\mu_f = 0.76$. The same deceleration may be obtained using a braking balance $\rho = 0.5$ (point B). In this case, even if the braking force is equally split between the front and rear wheel, the normalized braking force on the rear tire, $\mu_r = 1.20$, is much greater than the front one, $\mu_f = 0.38$. This is due to the load transfer effect. Interpreting the figure in a different manner, the deceleration $\ddot{x} = 0.6g$ may be achieved using a braking balance $\rho = 0.25$ (point C). In this case normalized braking forces are almost equal ($\mu_f = 0.57$ and $\mu_r = 0.60$), both tires are equally far from their friction limit and it may be asserted that braking forces are well balanced.

It may be observed that as the deceleration increases, the upper limit of the braking balance decreases, corresponding to predominant use of the front brake. Indeed, for a severe braking maneuver with a deceleration $\ddot{x} = g$, the braking balance may vary from $\rho = 0$ (point D) up to $\rho = 0.1$ (point E).

IDEAL BRAKING

A well balanced braking maneuver should engage the longitudinal adherence of both tires equally. In this manner the residual friction may be used for generating lateral forces which assist stability both in straight running and while cornering. A further advantage of this strategy is that both tires approach their friction limit simultaneously, thus it is possible to reach the maximum deceleration. In terms of normalized braking force, the ideal braking repartition corresponds to the diagonal of the friction rectangle represented in Figure 2 and described by the following equation:

$$\frac{\mu_f}{\mu_r} = \frac{D_f}{D_r} \tag{7}$$

Figure 2 shows that the ideal braking line is crossed by different braking balance curves. This means that the ideal value of braking balance depends on the deceleration, i.e. it depends on the total braking force. By assuming for simplicity that both tires have the same friction limit $D_f = D_r$ and by rearranging the equations of motion the following expression of the ideal braking balance is obtained:

$$\rho_{id} = \frac{a - h\dfrac{S_{tot}}{m\,g}}{a + b} \tag{8}$$

The expression above shows that the ideal braking ratio has a maximum value that corresponds to the weight repartition $a/(a+b)$. As the braking force increases, the ideal braking balance decreases and becomes zero in the stoppie condition. From equation (8), the following expressions of front and rear braking forces are obtained as:

$$S_f = \frac{m\,g\,b + S_{tot}\,h}{a+b}\,\frac{S_{tot}}{m\,g} \tag{9}$$

$$S_r = \frac{m\,g\,a - S_{tot}\,h}{a+b}\,\frac{S_{tot}}{m\,g} \tag{10}$$

The ideal braking curve corresponding to equations (9) and (10) is represented in Figure 3. As an example, let us assume that the braking traction coefficient is $D_r = D_f = 0.73$, which corresponds to the straight lines **RO** and **FO** for the rear and the front tire respectively. The admissible braking maneuvers (having $\mu < D$) are contained in the grey area of the plot. If only the rear brake is used, the maximum braking force is $S_{tot} = 766N$ and leads to a deceleration of $\ddot{x} = 0.285g$ (point R). If only the front brake is used, the maximum braking force is $S_{tot} = 1400N$ and leads to a deceleration of $\ddot{x} = 0.561g$ (point F). The use of the ideal braking repartition makes it possible to obtain a greater total braking force and deceleration (point **O**) $S_{tot} = 1950N$ and $\ddot{x} = 0.73g$. Figure 3 shows that the ideal value of the front braking force increases with the braking intensity. On the contrary, the ideal rear force grows until it reaches a maximum, then it decreases to zero under stoppie condition. Moreover, it may be observed that the rear braking force is always smaller than the front one.

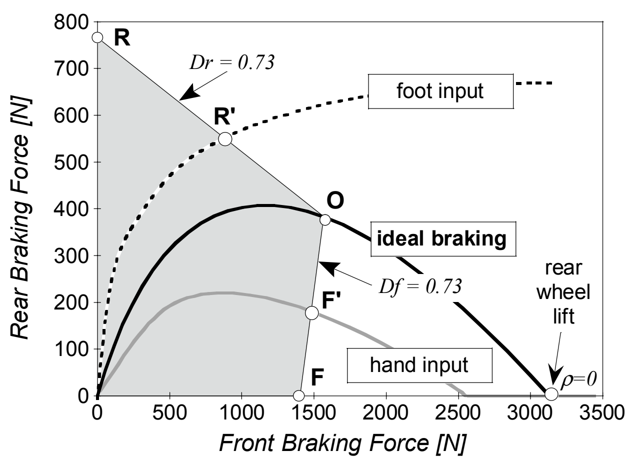

Figure 3 – optimal distribution of the braking force (m=274 kg, a= 0.741 m, b=0.682 m, h=0.643 m)

Figure 3 may be used for designing a combined braking system, which automatically distributes the total braking force between the two wheels. Indeed, dual combined braking systems are already implemented on commercial motorcycles. When the rider acts on the front-brake lever, the braking pressure is distributed on both the front and the rear calipers. Using this system, separate braking input are still necessary because the ideal braking ratio depends on the motorcycle load, which varies largely in presence of a passenger. The chosen pressure distribution produces a front force higher than the ideal case [3], so the actual braking distribution curve lies under the ideal braking curve of Figure 3. In a similar manner, when the rider pushes the rear brake pedal, the braking pressure is distributed on both brakes, keeping the rear braking force greater than the ideal case. Using the dual combined braking system, the rider still maintains the separate control of the front and rear brakes, but it is easy to achieve the more appropriate balance of braking force. Indeed, if only the hand input is used, the braking traction limit is reached in **F'** (braking force $S_{tot} = 1675N$), which is closer to the optimal braking point **O** than the point **F**. Similarly, if only the foot input is used, the braking traction limit is reached in **R'** (braking force $S_{tot} = 1445N$), which is closer to the optimal braking point **O** than point **R**. .

EFFECT OF DRAG FORCE

At high speed, drag force has a remarkable influence on motorcycle braking. However, aerodynamics force does not appreciably affect the considerations exposed above. By assuming for simplicity that the center of pressure coincides with the center of mass, the expressions of ideal braking balance (8), as well as the expression of braking force (9) and (10), are still valid. The only difference is that the presence of the drag force makes it possible to reach a greater deceleration, according to the following expression:

$$\ddot{x} = \frac{S_{tot} + F_D}{m} \tag{11}$$

IMPROVED ANALYSIS OF THE BRAKING MANEUVER

In this section the basic considerations exposed above are extended taking into account in detail the characteristics of tires and suspensions. Moreover, the out-of-plane stability of the vehicle is examined. For this purpose an eleven degree of freedom multibody model has been used. This model takes into account all relevant characteristics of a motorcycle, such as geometry, mass and inertia distribution, non-linear suspension and tire properties. The simulation code has been entirely developed at the Department of Mechanical Engineering (DIM) of the University of Padova [4], [5]. All motorcycle characteristics were measured at DIM for a sport motorcycle, including tire properties [6], [7]. The model has been successfully validated though comparison with experimental tests [5].

EFFECT OF THE BRAKING STYLE

A stopping maneuver at low speed was simulated. Starting from a speed of 15 m/s, a braking action was exerted on the vehicle in order achieve a maximum deceleration of 6 m/s^2. On dry asphalt with a braking friction coefficient $D_f = D_r = 1.4$, the motorcycle stops without tire skidding, regardless of whether it uses the ideal braking balance or only the front brake. On wet asphalt with one-half of the previous braking friction coefficient, only the ideal braking force distribution makes it possible to stop the motorcycle without wheel skidding. In this case, the use of only the front brake causes front wheel locking. This phenomenon occurs when the deceleration is about 5 m/s^2 and the speed is about 11.6 m/s, as shown in the Figure 4.

Figure 5 shows the longitudinal slip of tires during the maneuver. When only the front brake is used, front wheel locking occurs due to insufficient tire adherence. When the ideal braking force distribution is used, tire slip of both front and rear tires are almost equal, in accordance with the previsions of the simplified model.

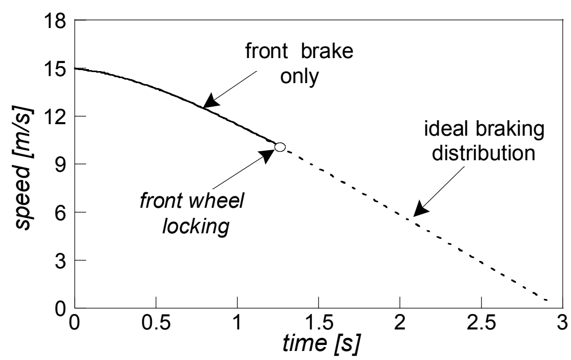

Figure 4 – stopping maneuver on wet asphalt

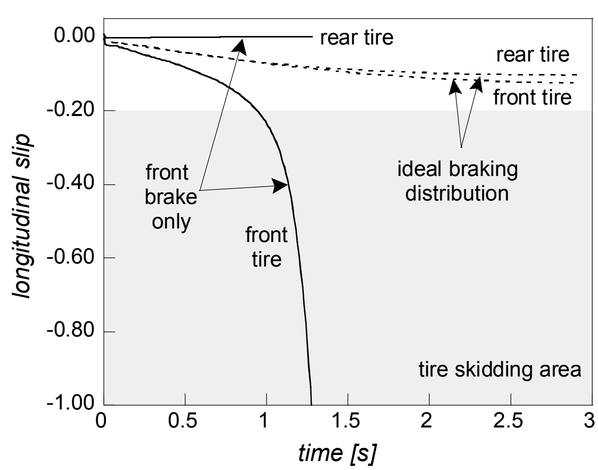

Figure 5 – tires longitudinal slip during the stopping maneuver

EFFECT OF THE SUSPENSIONS

Figure 6 shows the suspension travel during the maneuver. It may be observed that, using only the front brake, the front suspension is compressed and the rear one is totally extended. By using the ideal braking force distribution, the fork compression is reduced. More importantly, the extension of the rear suspension is also reduced, obtaining two positive effects. First, the motorcycle pitching is reduced. Second, the rear suspension remains inside its working range and it is still capable of absorbing road irregularities.

LATERAL STABILITY WHILE BRAKING

Two-wheel vehicles are intrinsically unstable because of their roll freedom. For a motorcycle, the main out-of-plane modes are the capsize, the weave, and the wobble mode, as reported in the literature [8], [9], [10], [11], [12]. Under braking conditions, the load transfer, the reduction of mechanical trail and caster angle, the variation of the cornering stiffness and lateral adherence, and the presence of braking forces affect the lateral stability of the vehicle. In next sections, motorcycle stability will be analyzed by means of numerical simulations. First the process of modeling the tire is briefly discussed, then root loci plots are presented showing the effect of the braking style.

TIRE MODEL

The behavior of tires when longitudinal slip, camber, and sideslip are simultaneously present is very complex [13], [14]. However, for analyzing the perturbation of motion under braking conditions a simplified tire model may be used. Indeed, the vertical load N and braking forces S are not affected by the small variations in the camber φ and sideslip angles λ. The following linearized expressions of the lateral force F and the yaw torque M_z may be used:

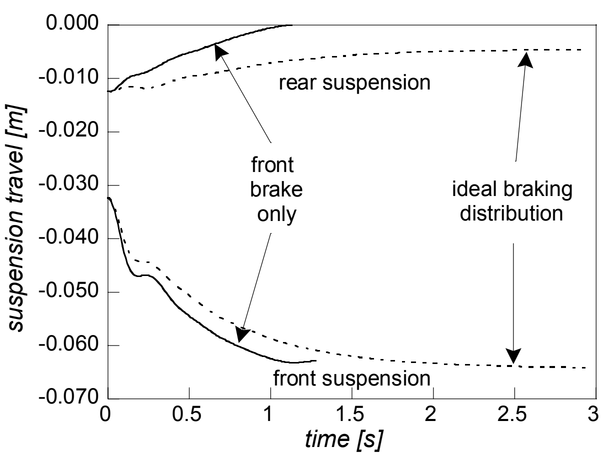

Figure 6 – suspension travel during the stopping maneuver

$$
\begin{aligned}
F &= K_\lambda(N,S)\lambda + K_\varphi(N,S)\varphi \\
M_z &= K_{SA}(N,S)\lambda + K_T(N,S)\varphi
\end{aligned} \tag{12}
$$

The relation between stiffnesses K and tire forces N and S are not linear, the following expressions are used for fitting measurements:

$$K_\lambda(N,S) = \alpha_\lambda \arctan(p_\lambda N)\left(1 - \frac{S}{D_x N}\right) \tag{13}$$

$$K_\varphi(N,S) = \alpha_\varphi N(1 + p_\varphi N)\left(1 - \frac{S}{D_x N}\right) \tag{14}$$

Figure 7 shows the measured data and the fitting curve of the cornering and camber stiffness for different tire loads. The cornering stiffness reduction due to the presence of the braking force is estimated. Yaw torque stiffnesses K_{SA} and K_T are fitted using formulas similar to expression (14).

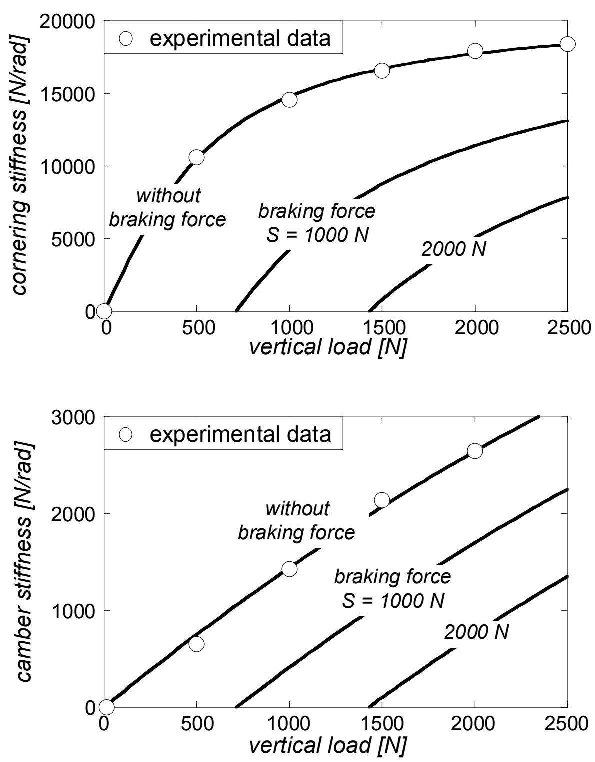

Figure 7 –cornering and camber stiffness of the rear tire as function of the vertical load and the braking force

LATERAL STABILITY

The Figure 8 shows the free-modes root loci in straight running for speeds from 5 to 50 m/s. The gray dots correspond to constant speed running, whereas the black dots are related to a deceleration of 4 m/s^2 and the black crosses correspond to a severe deceleration of 8 m/s^2. Simulations are repeated a) using the front brake

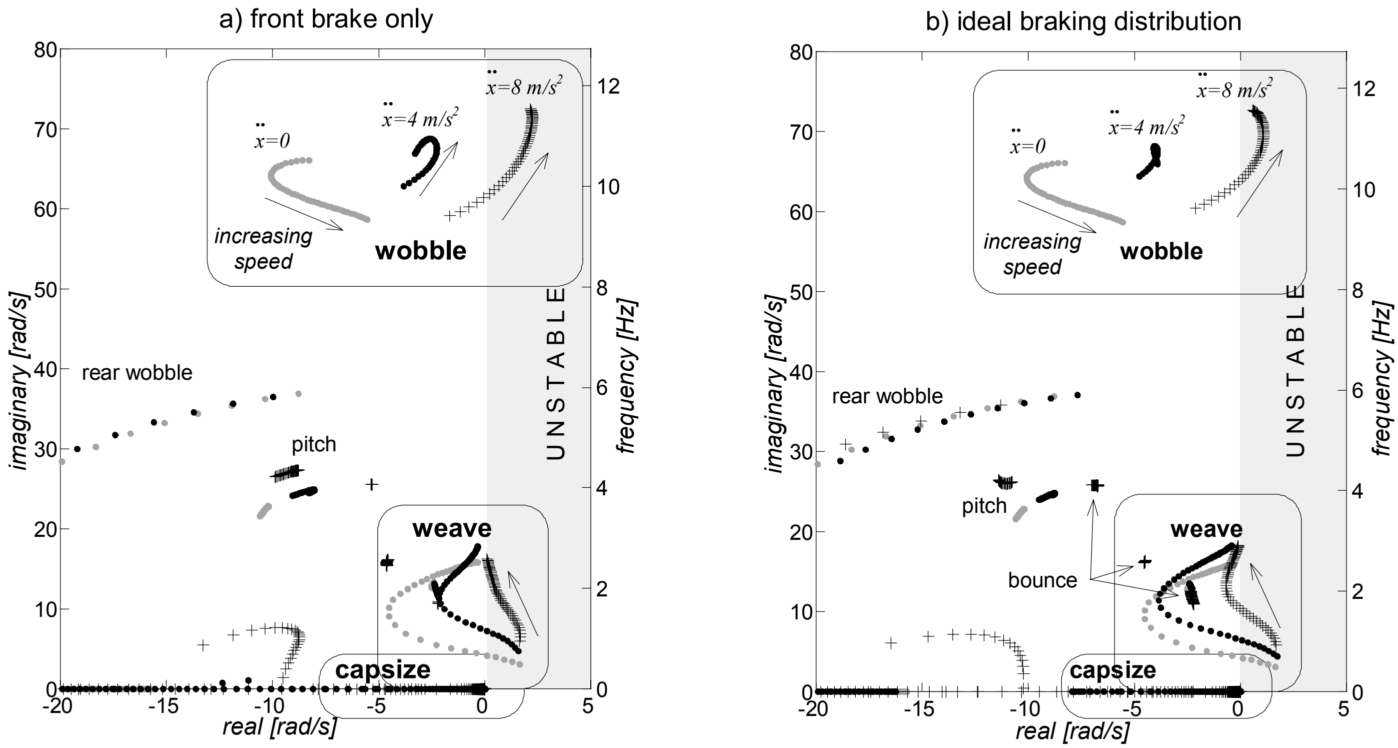

Figure 8 – Root loci in straight running (speeds from 5 up to 50 m/s, constant deceleration = 0, 4, and 8 m/s^2)

only and b) using the ideal braking balance. The eigenvalue analysis returns both the in-plane and out-of-plane modes. Since the first in-plane modes do not affect the vehicle's lateral stability, only weave, wobble and capsize modes will be discussed.

Regarding Figure 8a a number of observations can be made. Under constant speed conditions, the wobble mode has a frequency which decreases from 10.5 Hz at 5 m/s to 9.3 Hz at 50 m/s. The damping ratio is between 0.09 and 0.15. The deceleration of 4 m/s^2 mainly causes a decrement in the damping ratio, i.e. a reduction of the stability. The frequency at low speed is now lower than the frequency at high speed. The more severe deceleration of 8 m/s^2 causes a further decrement in the damping ratio and the wobble mode becomes unstable for speeds higher than 11 m/s. The weave mode stability displays a similar trend and it decreases as the deceleration increases. The weave mode at high deceleration is always unstable. At zero and medium deceleration, the weave mode has its maximum stability at medium speed. Capsize mode is stable in the whole range of speed and deceleration.

Figure 8b shows free modes under the same speed and acceleration conditions, but with the ideal distribution of braking force. It may be observed that this braking force balance has a positive effect on the stability. This is particularly evident for high speed wobble and the increment in damping ratio is higher at medium deceleration than at high deceleration. Indeed, severe decelerations produce high load transfer that reduces the braking capability of the rear tire. Figure 3 shows that in this condition the ideal braking maneuver is performed with the front brake only.

There are several reasons why the proper utilization of front and the rear brakes has a positive effect on vehicle stability under braking. In particular it may be observed that:

- As shown in the Figure 9, when straight running motion is perturbed, the torque generated by the front braking force and the inertial force tends to yaw the vehicle. On the contrary, the presence of a rear braking force generate a torque which tends to align and stabilize the vehicle [1].
- Tire trail has a positive effect on the wobble stability [1], [10]. The use of both brakes makes it possible to moderate the reduction of trail under braking. In the example considered, the vehicle has a nominal normal trail of 90 mm. At a deceleration of 4 m/s^2, when only the front brake is used, the trail is reduced to 80 mm whereas when both brakes are used it is 83 mm.
- As shown in Figure 7, cornering and camber stiffnesses vary as tire load and braking forces

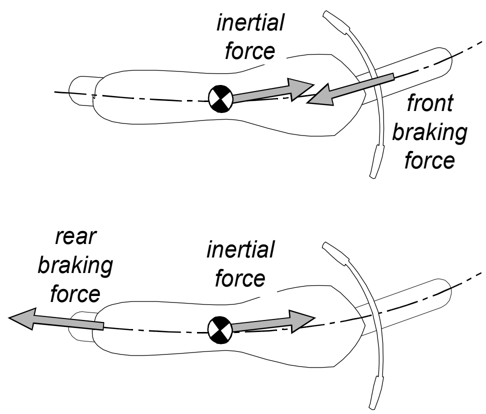

Figure 9 – yaw torques generates by braking forces

change. The ideal balance of the braking force makes it possible to moderate tire property variations and to achieve a well balanced vehicle under different motion conditions. For example, at a speed of 30 m/s and a deceleration of 4 m/s^2 obtained by using the front brake only, the cornering stiffnesses of front and rear tire are 22000 and 12000 N/rad respectively. The proper utilization of both brakes produces a lower front stiffnesses equal to 20200 N/rad and a higher rear stiffness equal to 17600 N/rad.

CONCLUSIONS

A detailed study of motorcycle behavior under braking conditions has been presented. A simplified model has been used for analyzing load transfer, rear wheel lift, and tire skidding phenomena as the deceleration varies. It has been shown that the maximum deceleration is limited by the vehicle mass distribution, the tire adherence, and the distribution of the braking force between the front and rear wheels. A strategy for optimizing braking performance has been explained. This strategy consists of always keeping the ratio between the front and rear braking force coefficients equal to the ratio between the front and rear longitudinal adherence limits. The advantages of this strategy are that both tires work equally far from their adherence limit. Thus, they have the same capability of generating additional forces and assuring vehicle stability and safety. Moreover, both tires approach their friction limit simultaneously, thus it is possible to achieve the maximum allowable deceleration. This strategy implies that when the braking force is low, it should be split between front and rear wheels. As the braking force increases, its main portion should be applied on the front wheel. This strategy may be used profitably with either high or low tire adherence. Braking maneuvers have been analyzed taking into account the suspension and tire properties. Multibody simulations, both on dry and wet roads, confirm the validity of the proposed braking strategy. The multibody model was then used for stability analysis. Root loci have been plotted for different speeds, deceleration rates and braking styles. It has been shown that the vehicle stability decreases as the deceleration rate grows. In this scenario, the choice of the ideal braking balance has a remarkable stabilizing effect on the stability of weave and wobble modes.

ACKNOWLEDGMENTS

This research was partially supported by funds from the Italian Ministry for Universities and for Scientific and Technological Research (MURST 40% funds).

REFERENCES

[1] V. Cossalter: “Motorcycle Dynamics”, Race Dynamics, Milwaukee, USA, 2002

[2] H.B. Pacejka and E. Bakker: The Magic Formula Tyre Model. Vehicle System Dynamics 21 (1991), pp. 1–18.

[3] M. Kato, T. Matsuto, K. Tanaka, H. Ishihara, T. Hayashi, W. Hosoda: Combination of antilock brake system (ABS) and combined brake system (CBS) for motorcycles. SAE Special Publications, n. 1142, Current and Future Developments in ABS/TCS and Brake Technology, 1996, p 59.

[4] V. Cossalter and R. Lot: A Motorcycle Multi-Body Model for Real Time Simulations Based on the Natural Coordinates Approach, Vehicle System Dynamics Vol 37, n.6, June 2002, pp. 423–448.

[5] V. Cossalter, R. Lot and F. Maggio: A Multibody Code for Motorcycle Handling and Stability Analysis with Validation and Examples of Application , SAE paper 2003–32–0035, SETC 2003.

[6] V. Cossalter, A. Doria, and R. Berritta: Identification of the Lateral and Cornering Stiffness of Scooter Tyres Using Impedance Measurements, Proceedings of 2nd Int. Conf. on Identification in Engineering Systems, Swansea, 28–31 March,1999

[7] V. Cossalter, A. Doria, R. Lot, N. Ruffo and M. Salvador: Dynamic Properties of Motorcycle and Scooter Tires: measurement and comparison, Vehicle System Dynamics Vol 39, n.5, May 2003, pp. 329–352.

[8] R. S. Sharp: “The Stability and Control of Motorcycles”, Journal of Mechanical Engineering Science, Vol. 13 (1971).

[9] C. Koenen and H. B. Pacejka: “Vibrational Modes of Motorcycles in Curve”, proc. Int. Motorcycle Safety Conf. Washington D.C., (1980).

[10] V. Cossalter, R. Lot, F. Maggio: The Influence of Tire Properties on the Stability of a Motorcycle in Straight Running and Curves, SAE Dynamic and Stability Conference, May 7–9, 2002, Detroit, proceedings.

[11] V. Cossalter R. Lot and F. Maggio: The Modal Analysis of a Motorcycle in Straight Running and on a Curve, Meccanica, Kluwer ed, (2003)

[12] D.J.N Limebeer, R.S. Sharp, S. Evangelou: The stability of motorcycles under acceleration and braking, Journal of Mechanical Engineering Science, v 215, n 9, 2001, pp. 1095–1110

[13] De Vries, E.J.H. and Pacejka, H.B.: Motorcycle tyre measurements and models. Proc. 15th IAVSD symposium: The dynamics of vehicles on road and tracks, Budapest, Hungary, (1997), pp. 280–298.

[14] R. Lot: A Motorcycle Tire Model for Dynamic Simulations: Theoretical and Experimental Aspects, Meccanica Vol 39, n. 3, pp. 204–218.

CONTACT

Eng. Roberto Lot
Dept. of Mechanical Engineering, University of Padova
Via Venezia 1, 35131 Padova (Italy)
e–mail: roberto.lot@unipd.it
www.dinamoto.it